

1 **A methodological roadmap to quantify animal-vectorized spatial ecosystem subsidies**

2

3 Diego Ellis-Soto^{1,2+}, Kristy M. Ferraro³⁺, Matteo Rizzuto⁴, Emily Briggs^{3,5}, Julia D. Monk³, Oswald
4 J. Schmitz³

5

6 1 Department of Ecology and Evolutionary Biology, Yale University, New Haven, CT, USA

7 2 Center for Biodiversity and Global Change, Yale University, New Haven, CT, USA

8 3 School of the Environment, Yale University, 370 Prospect Street, New Haven, CT, USA

9 4 Department of Biology, Memorial University of Newfoundland St. John's, Canada

10 5 Department of Anthropology, Yale University, New Haven, CT, USA

11 Corresponding author: diego.ellissoto@yale.edu

12

13 + These authors contributed equally to this work

14

16 **Keywords:** Meta-ecosystem theory, animal movement, biogeochemistry, ecosystem ecology,
17 stoichiometry, remote sensing

18

19 **Abstract**

20
21
22
23
24
25
26
27
28
29
30
31
32
33
34
35
36
37
38
39
40
41
42
43

Ecosystems are open systems connected through spatial flows of energy, matter, and nutrients. Predicting and managing ecosystem interdependence requires a rigorous quantitative understanding of the drivers and vectors that connect ecosystems across spatio-temporal scales. Animals act as such vectors when they transport nutrients across landscapes in the form of excreta, egesta, and their own bodies. Here, we introduce a methodological roadmap that combines movement, foraging, and ecosystem ecology to study the effects of animal-vectored nutrient transport on meta-ecosystems. The meta-ecosystem concept — the notion that ecosystems are connected in space and time by flows of energy, matter, and organisms across boundaries — provides a theoretical framework on which to base our understanding of animal-vectored nutrient transport. However, partly due to its high level of abstraction, there are few empirical tests of meta-ecosystem theory, and while we may label animals as important mediators of ecosystem services, we lack predictive inference of their relative roles and impacts on diverse ecosystems. Recently developed technologies and methods — tracking devices, mechanistic movement models, diet reconstruction techniques and remote sensing — have the potential to facilitate the quantification of animal-vectored nutrient flows and increase the predictive power of meta-ecosystem theory. Understanding the mechanisms by which animals shape ecosystem dynamics may be important for ongoing conservation, rewilding, and restoration initiatives around the world, and for more accurate models of ecosystem nutrient budgets. We provide conceptual examples that show how our proposed integration of methodologies could help investigate ecosystem impacts of animal movement. We conclude by describing practical applications to understanding cross-ecosystem contributions of animals on the move.

44 **Introduction**

45

46 **Ecosystems and animal nutrient cycling**

47

48 Flows of energy, nutrients, matter, and organisms crisscross landscapes worldwide, connecting
49 intrinsically open ecosystems over space and time. The advancement of meta-ecosystem
50 theory (Loreau *et al.* 2003; Leroux & Loreau 2008; Massol *et al.* 2011; Marleau *et al.* 2014) has
51 aided our understanding of the influence of these spatial exchanges in both donor and recipient
52 ecosystem functioning (Gounand *et al.* 2018b). Classic ecosystem theory holds that the spatial
53 flow of organic and inorganic matter from source to recipient locations is largely passive, coming
54 for example from *in situ* weathering of parent geological material, release from riverine
55 sediments, wind-born dust, or rain-driven and snowmelt-driven run-off (Chapin *et al.* 2012).
56 Nevertheless, there is growing appreciation that ecosystems also receive subsidies via animal
57 movement (Vanni, 2002; Atkinson, Capps, Rugenski, & Vanni, 2017; Schmitz *et al.*, 2018;
58 McInturf, Pollack, Yang, & Spiegel, 2019). Such movement can result in an influx of new prey or
59 predators to recipient locations, pulses of animal-transported nutrients in dung and urine, or the
60 accumulation of organic matter via decomposition of carcasses deposited in recipient locations
61 (henceforth, animal-vectored subsidies; Earl & Zollner 2017; McInturf *et al.* 2019). Whenever
62 biotic—such as animal-vectored subsidies—or abiotic processes influence the structure and
63 functioning of ecosystems, they are deemed ecosystem controls (Weathers *et al.* 2012). Theory
64 predicts that animals can exert top-down control on ecosystems via subsidies, the magnitude of
65 which could sometimes be equal to bottom-up (Leroux & Loreau, 2008; Allen & Wesner, 2016).

66

67 Increasingly, migratory populations of large bodied species are recognized for playing an
68 especially important role as landscape-scale vectors of ecosystem subsidies (Bauer & Hoyer
69 2014). Yet at the same time, across the globe, their populations are in decline (Wilcove &
70 Wikelski 2008; Dirzo *et al.* 2014) and their movement is increasingly constrained by human
71 activities (Tucker *et al.* 2018). The implications of such effects on top-down control over
72 ecosystem functioning at broad spatial scales remain uncertain, but estimates suggest they can
73 be substantial (Doughty *et al.* 2016). Hence, an important avenue of new research in ecosystem
74 ecology is empirically resolving the relative importance of animal-vectored vs. passive subsidies
75 on ecosystem functioning. We are at an opportune scientific and technical juncture to begin
76 synthesizing advances made in disparate fields.

77

78 The empirical challenge in understanding and attributing how much control animals exert over
79 ecosystem functioning is to quantify spatial flows of different kinds of animal-vectored subsidies
80 (i.e. excretion, egestion, carcass deposition, reproductive material). While theory is in place to
81 identify the different components that need measuring to obtain a coherent understanding of this
82 phenomenon (Leroux & Loreau, 2008; Earl & Zollner, 2017; Gounand et al. 2018; Schmitz et al.,
83 2018), it remains largely conceptual and offers few insights into how to operationalize empirical
84 measurement. Here, we address this limitation by offering a methodological road map that
85 discusses the various measurements that need to be integrated to develop a coherent picture of
86 the quantitative effects of animals on nutrient dynamics across ecosystems. There is now
87 unprecedented ability to characterize functional and structural properties of ecosystems
88 including topography, vegetation community composition, and habitat structure across vast
89 spaces (Bergen *et al.* 2009; Pettoirelli *et al.* 2018). Likewise, movements of a wide range of
90 animal species can be monitored remotely (Kays, Crofoot, Jetz, & Wikelski, 2015; Wilmers et
91 al., 2015a), which can facilitate quantification of the net effects of animals on nutrient and
92 material transport. New DNA-based and isotopic analyses can resolve dietary nutrient sources.
93 Additionally, these nutrient sources and fates can be mapped spatially using nutrient distribution
94 modeling (West et al. 2010; Sitters *et al.* 2015; Leroux *et al.* 2017). While ripe for integration,
95 these methods and technologies continue to be deployed separately in research that examines
96 different components of animal movement and resource use within ecosystems. We show here
97 how these different methods can be used jointly to give a coherent, theory-driven understanding
98 of the ecosystem consequences of animal-vectored nutrient flows across landscapes.

99

100 **Materials and Methods**

101

102 **Meta-ecosystem models to understand animal-vectored subsidies**

103

104 The series of measurements we discuss are motivated by ecological theory on meta-ecosystem
105 dynamics. A multitrophic version of such an ecosystem model can be used to consider how
106 internal dynamics of ecosystems are connected by regional flows of materials and organisms
107 between the ecosystems (Marleau *et al.* 2014). To identify the processes that need to be
108 measured, we consider a model configured as a four trophic level food chain (Fig. 1), which
109 describes the dynamics of a single abiotic nutrient or element (N), a plant (P), a herbivore (H),
110 and a carnivore (C) within and between i local ecosystems that together create the meta-
111 ecosystem. This structure is intended for simple illustrative purposes to show how to relate the

112 dynamical systems model to the salient ecosystem and spatial processes that need to be
113 measured. The model can be made more complex by considering multiple nutrients to make it
114 stoichiometrically explicit (Leroux *et al.* 2012; Cherif & Loreau 2013) as well as multiple species
115 among trophic levels (McCann *et al.* 2005). Such granularity is beyond the scope of this paper.
116 Instead, we use this theoretical framework specifically to identify salient processes (and inherent
117 variables) that need to be measured to obtain a quantitative understanding the role of animals in
118 connecting and shaping the structure and functioning of local ecosystems across spatial scales.
119 The model reveals two salient processes that need to be considered: trophic interactions and
120 nutrient translocation and deposition. These two processes can be subdivided into five more
121 finely resolvable spatial components (Fig.1) that require detailed measurement. Hence, our
122 roadmap focuses on measuring these five components.

123
124 Trophic interactions within ecosystem i determine nutrient uptake and assimilation by
125 herbivores and carnivores (Fig. 1) that may vary in size, and habitat structure within an
126 ecosystem determines species spatial occurrences and the nature of their interactions (Schmitz
127 *et al.* 2017). Thus, an accounting of animal spatial interactions will require analysis of: (1) the
128 spatial extent and spatial grain size for analysis of the focal animal species and their
129 interdependent predators or prey/resources (i.e., spatial trophic food chain structure) in relation
130 to (2) the habitat structure within and between source and recipient local ecosystems. Moreover,
131 animals can be selective in their choice of resources, necessitating further spatial analyses of
132 (3) the resources selected by animals in source and recipient locations. Nutrient translocation
133 and deposition in ecosystems will depend on (4) the movement rates and directional spatial
134 flows of animal species and animal-vectored nutrients, and (5) the amounts and spatial
135 deposition rate of animal transported nutrients or materials, which can include the animals' own
136 body mass, waste products, reproductive material, and dispatched prey. Each of these
137 components can be measured with its own set of technologies (Fig. 2). We next provide a brief
138 review of these tools and of their potential use in the context of measuring animal-vectored
139 subsidies.

140

141 **(1) Spatial trophic structure**

142 The first step to understanding how animal movement shapes ecosystems is to describe the
143 geographic domain over which focal animals roam and their trophic position within food chains,
144 including the scope of interactions with predators and resources (Fig. 2). These factors will
145 determine the geographic area and spatial grain of interest, the animals' habitat domain within

146 that area, and any ecosystem effects the animal could have within said domain through
147 cascading impacts on associated food webs. The habitat domain is the spatial extent of habitat
148 space used within a species' broader home range that is relevant to interspecific interactions,
149 e.g., areas used for foraging or avoiding predation (Schmitz *et al.* 2017).

150
151 Characterizing the spatial grains at which animals interact with other species and their
152 environment is crucial to understanding their distributions. Animal movement can be described
153 at fine spatial scales (e.g. responses to environmental resources such as foraging [see section
154 3]) or at coarser scales, such as their broad home range (introduced in section 4) (Mertes *et al.*
155 2020). Fine and coarse spatial grains have been termed "response grain" and "occupancy
156 grains", respectively (Mertes *et al.* 2020). To quantify an animal's response grain, first passage
157 time analysis can be employed. These are defined as the time it takes an animal to cross a
158 circle with a defined radius -- and as such scale dependent -- and can quantify the time duration
159 of an individual animal present within such a circle (Fauchald & Tveraa 2003). First passage
160 time allows estimating the spatial scale at which an individual animal focuses its search efforts
161 (i.e. by plotting variance in first passage time against the spatial scale, Fauchald & Tveraa 2003,
162 Fig. 2 bottom left panel). As such, hierarchical scales of animal habitat selection (Johnson 1980;
163 Mertes & Jetz 2017; Mertes *et al.* 2020) should drive the spatial resolution of remote sensing
164 products selected for analysis, not the other way around. This is especially relevant for animal
165 movement data, which are typically measured at finer spatio-temporal resolutions than data
166 from remotely sensed imagery (Remelgado *et al.* 2017, 2019). The habitat domain can be
167 measured using movement data by tracked individuals across a landscape, to calculate an
168 animals utilization distribution and probabilities of spatial locations associated with foraging and
169 migration behaviour across a landscape (Schmitz *et al.* 2017). A three-dimensional utilization
170 distribution could be estimated if vertical movements are tracked, e.g. movement in forest
171 canopies (McLean *et al.* 2016).

172
173 Species interactions can alter animal movement behaviour, which can in turn impact ecosystem
174 nutrient dynamics (Schmitz, Hawlena, & Trussell, 2010; Schmitz *et al.*, 2018). Hence
175 consideration of the amount and spatial domain of animal vectored subsidies needs to consider
176 species embeddedness within food chains. Moreover, such consideration will enhance the
177 appreciation that animal vectored subsidies can trigger the rearrangement of food chains or
178 initiate novel trophic interactions (Montagano *et al.* 2019). Generally in this context, primary
179 producers have a trophic position of 1, primary consumers have a trophic position of 2,

180 secondary consumers have a trophic position of 3, and so on (Leroux & Loreau 2012). Yet there
181 are many animals that occupy trophic positions between these discrete designations. For
182 example, an omnivore may consume mostly primary consumers, but also some secondary
183 consumers and therefore have a trophic position between 2 and 3 (Kelson et al 2020). We
184 discuss how stable isotopes may be used to determine trophic position in section 3, which is
185 important to resolve the nature and source of nutrients (e.g. largely plant-based vs. largely
186 animal-based) that comprise subsidies (see section 3, Kelson et al. 2020).

187

188 ***(2) Habitat structure within and between source and recipient locations***

189

190 Habitat structure and topographic features, within and between source and recipient locations,
191 shape animal movement and nutrient transport within habitat domains (Leroux & Loreau, 2008;
192 Gounand, Little, Harvey, & Altermatt, 2018; Schmitz et al., 2018). A spatially accurate
193 characterization of these fundamental ecosystem attributes is key to understanding why, how,
194 and where animals move over the landscape (Fig. 2). Earth observation via satellite, airborne,
195 or drone imagery provides an important basis for developing such a characterization (Allan *et al.*
196 2018; Pettorelli *et al.* 2018). Remotely sensed landcover maps (i.e. forest, grassland, urban) can
197 be used to delineate ecosystem boundaries and assess how these change through time.
198 Advances of LiDAR (Light Detection and Ranging) make it possible to characterize vertical
199 habitat structure and above-ground vegetation biomass within and across ecosystem
200 boundaries. Furthermore, ecosystem productivity can be remotely measured and represented
201 as vegetation indices (de Araujo Barbosa *et al.* 2015; Pettorelli *et al.* 2018). Topographic
202 products, such as slope and topographic ruggedness (Amatulli *et al.* 2018), can resolve passive
203 abiotic flow pathways to pinpoint where nutrients may end up on the landscape (e.g., flow down
204 concave and into convex surfaces; Lindeman, 1942; Leroux & Loreau, 2008). Finally, LiDAR
205 estimates are becoming available from the Global Ecosystem Dynamics Investigation (GEDI)
206 mounted on the International Space Station, which measures forest structure and above-ground
207 biomass density across the globe (Hancock *et al.* 2019)

208

209 More finely resolved structure can be obtained within habitats using hyperspectral technologies
210 to collect hundreds of bands across the electromagnetic spectrum which distinguish unique
211 'fingerprints', referred to as spectral signatures for different kind of environmental features
212 (Stuart *et al.* 2019). Such spectral signatures can be related to spatial patterns in plant
213 functional diversity, vegetation elemental composition, and plant density (Knyazikhin *et al.* 2013;

214 Jetz *et al.* 2016; Schneider *et al.* 2017; Durán *et al.* 2019). Further, endmember extraction from
215 multispectral imagery can be used to extract information on subpixel features, e.g., to identify
216 signatures of water availability and abundance (Xie *et al.* 2016) .

217
218 Remotely sensed environmental products have different pixel resolution, commonly referred to
219 as 'grain size'. Accessing and utilizing a plethora of remote sensing products is facilitated
220 through geoprocessing tools such as Google Earth Engine, the Movebank Env-Data system,
221 and the getspatialdata package (Pettorelli *et al.* 2014; Clark *et al.* 2016; Wegmann 2017). We
222 list a collection of remote sensing products available to study ecosystem features across source
223 and recipient locations in Table 1. Regardless of the product used, coherent understanding
224 requires a grain size that aligns with the grain size of measurement of animal movement.

225 226 **(3) Resources available to and selected by animals in source and recipient locations**

227
228 Characterization of species habitat domains and structure can next be used to determine why
229 animals move where they do, and what resources they use in source and recipient locations
230 (Fig. 2). This can be accomplished using resource selection functions (RSF; Boyce *et al.* 2002)
231 and step selection functions (SSF; Fortin *et al.* 2005). Generally, these functions associate
232 environmental variables with locations used by individual animals and compare these with
233 randomly generated points representing locations available to, but not used by, them (Michelot
234 *et al.* 2019). Both methods estimate the probability of animal presence as a function of
235 environmental covariates. SSF can be used further to predict future movement paths of animals,
236 while RSF predicts spatial patterns of species occurrences over spatio-temporal scales
237 (Michelot *et al.* 2019). Parameters from SSF can highlight whether animals avoid or are
238 attracted to certain landscape features or resources. For example, SSF analysis reveals that in
239 Etosha National Park, Namibia, elephants avoided areas with high tree biomass and were
240 attracted to water sources and grassland patches with long term patterns of productivity
241 (Tsalyuk *et al.* 2019). This could indicate that waterholes and grasslands receive more animal-
242 vectored subsidies from elephants when compared to steep areas or dense forests. Such
243 behavioural information would improve mechanistic predictions of nutrient redistribution by
244 these wide-ranging megafauna which are known to play a large effect on regional carbon
245 budgets (Berzaghi *et al.* 2018).

246

247 Resource selection is a hierarchical process (Courbin et al. 2013). While RSF and SSF are
248 broad-scale measures of animal movement and habitat use, more finely resolved measures are
249 needed to understand which food items are used by animals and their nutritional values within
250 different locations. This understanding of animal food consumption and eventual processing and
251 deposition (in body material, or as urine and fecal matter) can provide an understanding of
252 where and how nutrients removed from donor ecosystems end up in recipient ecosystems.
253 Additionally, the identity of consumed resources directly impacts the quantity and quality of
254 nutrients deposited by animals (Subalusky & Post 2018).

255
256 Traditionally, dietary analyses have been performed based on physical dissection and
257 microhistological analyses of stomach contents and fecal matter (Holechek et al., 1982, Joly,
258 2018). These methods, however, often require either opportunistic sampling of carcasses or
259 destructive harvesting of live animals. DNA-metabarcoding provides an alternative, as it allows
260 for the identification of materials consumed using fecal matter alone (Kartzinel et al. 2015; see
261 Deagle et al., 2019 for an overview of DNA-metabarcoding methods). DNA-metabarcoding can
262 shed important insights into the trophic ecology of source and recipient sites, and how
263 consumption, and thus acquisition and transport of nutrients, can change in time and space
264 (Pansu et al. 2019). For example, Atkins et al. (2019) combined GPS tracking data of bushbuck
265 (*Tragelaphus sylvaticus*) with DNA-metabarcoding of fecal samples to show that herbivores
266 occupy new habitats and forage on novel food items after extirpation of their predators.
267 Bushbuck presence further changed plant community composition (demonstrated by comparing
268 plant composition in exclosure and control plots) (Atkins et al. 2019). A playback experiment of
269 predator sounds was able to revert bushbuck behaviour as they perceived predation risk (Atkins
270 et al. 2019).

271
272 Stable isotopes, such as $\delta^{15}\text{N}$, $\delta^{13}\text{C}$, and $\delta^{18}\text{O}$, are also powerful tools in elucidating the trophic
273 position (Ben-David et al., 2012), diet, and foraging location of a focal species in a non-invasive
274 manner (Newsome et al. 2010; Kristensen et al. 2011). In general animals are enriched by $\sim 3\%$
275 of nitrogen and $\sim 1\%$ of carbon compared to what they eat, providing an estimate of trophic
276 position (Post 2002). Therefore, trophic position can be discerned by using the isotopic
277 signature (i.e. $\delta^{15}\text{N}$) of the consumer, of the ecosystem's primary producers, and a
278 discrimination factor for the change in $\delta^{15}\text{N}$ enrichment between the ecosystem's trophic levels
279 (Kelson et al. 2020). Using stable isotopes could also be a cost-effective way to identify the
280 correct primers when conducting DNA-metabarcoding. For example, while white-tailed deer are

281 primarily herbivores, there is some evidence that they sometimes consume animal matter (Ellis-
282 Felege *et al.* 2008). If stable isotopes revealed that deer have an omnivorous diet, DNA-
283 metabarcoding could be used to discern exactly what animal material they consumed.

284

285 Stable isotopes can also be used to arrive at approximate estimates of diet. The isotopic
286 signatures of food items (for example, C3 and C4 plants) often vary from one another.
287 Therefore, examining the isotopic signature in bone, tooth, or feces has shown a successful
288 method of coarsely understanding diet (Ben-David & Flaherty 2012). We recommend using
289 stable isotopes to determine diet if DNA-metabarcoding is not financially possible, when using
290 samples that have degraded and DNA-metabarcoding is no longer possible, or when a broad
291 understanding of diet is sufficient for the question at hand For an extensive overview of using
292 stable isotopes for ecological research, see Ben-David & Flaherty (2012), Hobson *et al.*, (2019),
293 and West *et al.* (2010).

294

295 **(4) The movement rates and directional patterns of animal species and subsequently** 296 **translocated nutrients**

297

298 Animals can transport nutrients along and against biophysical gradients (Earl & Zollner, 2017;
299 McInturf *et al.*, 2019). Therefore, an understanding of animal movements will elucidate the
300 nature and scale of consequent nutrient transfer (Fig. 2). Patterns of animal movement are
301 directly related to the degree of connectivity (c_{ij} , Fig. 1) among local ecosystems as well as the
302 movement rates of the animals (d_H , d_C , Fig. 1), which depend on the topography of the
303 biophysical gradient. Advances in animal tracking technologies – dubbed biologging – offer
304 possibilities to study internal (e.g., physiology, metabolism, reproduction) and external (e.g.,
305 social, environmental) drivers of animal movement (Nathan *et al.* 2008). Biologging enables
306 quantification of the space-use and resource requirements of animals (Kays *et al.* 2015; Hays *et*
307 *al.* 2019). The frequency with which animals visit certain areas (e.g., waterholes, fruit bearing
308 tree, latrines) can be estimated via first passage times and recursive analysis (Mahoney &
309 Young 2017; Bracis *et al.* 2018; Mertes *et al.* 2020).

310

311 Migrations are among the greatest examples of animal movement. Extensive research has
312 explored their direction, length, and drivers (Dechmann *et al.* 2017; Somveille *et al.* 2018, 2019).
313 Locations of an animal's track can be classified into specific movement strategies (i.e. disperser,
314 migrator, nomad, central place forager) by segmentation methods (Bastille-Rousseau *et al.*

315 2016; Edelhoff *et al.* 2016), thus setting the stage for further analysis. Fine-scale animal
316 behaviour (i.e. foraging, rest, travel) can be resolved in GPS data using behavioural change
317 point analysis, expected-maximum binary clustering methods (Garriga *et al.* 2016), and state-
318 space models (Patterson *et al.* 2008). A promising approach combining state-space and
319 continuous time correlated random walk models (Michelot & Blackwell 2019) allows estimating
320 behavioural states when using tracking data that are not sampled at regular time intervals,
321 which is a common occurrence with biologging data.

322

323 Modern biologging tags are comprised of GPS units, accelerometers, and additional on-board
324 sensors. Accelerometers estimate change in velocity of body postures over time and can
325 classify behavioural states of wild animals, including hunting, killing, resting (Brown *et al.* 2013;
326 Williams *et al.* 2014), and even scent marking (Bidder *et al.* 2020). Accelerometers also allow
327 quantifying energy expenditure of animals and of specific behaviours. Common methods for
328 such energy expenditure are two closely linked metrics; Overall Dynamic Body acceleration
329 (ODBA) and Vectorized sum of the Dynamic Body Acceleration (VeDBA) (Wilson *et al.* 2006,
330 2020). We refer to Joo, Boone, Clay, & Patrick, (2019) for a review on animal movement
331 analysis.

332

333 Movement ecology increasingly studies fine scale behaviours such as foraging or sociality
334 (Strandburg-Peshkin *et al.* 2015; Bennison *et al.* 2018) that can determine fine scale spatial
335 heterogeneity in nutrient release, a process not yet considered in the current literature on
336 animal-vectored subsidies (Gounand *et al.* 2018b). At the same time, movement ecology rarely
337 quantifies the scale, scope, and magnitude of animal-mediated nutrient transfers.

338

339 **(5) *The amounts and deposition rate of animal transported nutrients or material***

340

341 Remote sensing offers quantitative measures of ecosystem structure at broad geographic
342 scales. Collecting environmental data in the field provides detailed information that is essential
343 and complementary to remote sensing to understand how local microclimate influences
344 ecosystem dynamics and the distribution of animals and the resources they consume
345 (Zellweger *et al.* 2018) (Fig. 2, right panel). Local observations identify how trophic interactions
346 and community structure vary across habitats and environmental gradients. For example, one
347 could measure a site's microtopography (slope, elevation, roughness), surrounding vegetation
348 type and cover. The development of methods to account for such micro-environmental variation

349 is necessary to facilitate realistic representations of environmental conditions experienced by
350 organisms. Downscaled remote sensing products show promise in providing such fine spatial
351 detail (Maclean *et al.* 2019; Maclean 2020) and, once overlaid with animal locations, enable
352 identification of habitats that are source and recipient locations for animal-vectoring nutrient
353 subsidies.

354
355 Animal vectoring subsidies involve several processes, including consumption, excretion,
356 egestion, and deposition of carcasses and parturition material (McSherry & Ritchie 2013;
357 Subalusky & Post 2018; Wenger *et al.* 2019). For example in the Maasai Mara National Park
358 Reserve, Kenya, every day Hippopotamus egest approximately 36 tons of wet biomass
359 consumed in terrestrial ecosystems into the Mara river, approximately 15 % of the dissolved
360 organic carbon loading from the upstream catchment (Subalusky *et al.* 2015). Also in the Mara,
361 mass drowning of wildebeest contributes ~18% of the total dissolved organic carbon to the river
362 ecosystem (Subalusky *et al.* 2017).

363
364 Standard biogeochemical methods, which include analyses that quantify elemental composition
365 of materials, can be used to characterize the stoichiometry and total nutritional composition of
366 food items (Vanni *et al.*, 2002). Additionally, these methods can assess nutrient quality and
367 quantity of animal-deposited material (e.g. egesta, excreta, carcasses) as well as the magnitude
368 of nutrient influx into the surrounding environment through *in situ* measurement of various soil
369 and plant properties (e.g., pH, soil texture, plant community composition, soil and plant nutrient
370 content) at sites of animal activity (i.e. see Bump *et al.*, 2009, Risch *et al.* 2020). Finally, given
371 that stable isotopes that come from animal tissues and excreta are isotopically enriched
372 compared to their diet, enriched plant and soil materials surrounding the deposition can indicate
373 deposition and use of animal-vectoring subsidies (Bump *et al.* 2009a). Such enrichment may
374 also help parse out passive from active subsidy input.

375
376 The tracing and mapping of spatial nutrient flows and deposition can be aided by using
377 stoichiometric distribution models (StDMs). Such models predict the geospatial distribution of
378 nutrients in forage items (Leroux *et al.* 2017). Similar to a species distribution model and point
379 Poisson process models, a resource – in this case a forage item's nutrient content, either
380 absolute (g/m^2 ; i.e. quantity) or relative (carbon:nitrogen ratio; i.e. quality) – can be defined as
381 the abundance of a given nutrient (nitrogen, phosphorus or carbon) in location x_i which is
382 predicted by a vector of environmental covariates $z_{(x_i)}$, their coefficients β_i , and an error term \mathcal{E} .

383 StDMs map the distribution of nutrients in ways that can be overlaid with animal spatial habitat
384 domains, to reveal how animals respond to spatial variation in resource distribution across a
385 landscape (Leroux *et al.* 2017) and may create microsites of heterogeneity where subsidies are
386 transported against stoichiometric gradients in the broader landscape.

387

388 **From diverse data sources, to a coherent message - A road map for integrating methods**

389 The current technological and methodological juncture allows us to go beyond understanding
390 the drivers of animal movement. We now have the tools to enhance our understanding of the
391 ecosystem-wide consequences of animal movements, generating inference on the timing,
392 directionality, and magnitude of animal mediated subsidies on both donor and recipient
393 ecosystems. Our road map identifies five steps needed to develop such a coherent picture and
394 is presented in Figure 2. We illustrate the value of this road map with two case studies, one of a
395 herbivore and one of a top predator, discussing how methods from these five steps can be
396 integrated to understand how animals on the move influence their ecosystems at fine scales.

397

398 **Case Studies**

399 **Measuring nutrient loading by Galapagos tortoises during their seasonal migration**

400 Galapagos tortoises (*Chelonoidis porteri*) are ecosystem engineers due to their seed dispersal
401 abilities, trampling of vegetation, and transport of nutrients (Gibbs *et al.* 2010; Blake *et al.* 2012;
402 Ellis Soto 2020). Coupling tortoise tracking data with remotely sensed NDVI has identified that
403 giant tortoises undergo seasonally recurring migrations in response to averages of long-term
404 environmental conditions (Bastille-Rousseau *et al.* 2019). Behavioural observations revealed
405 that tortoises preferentially feed on an agricultural crop (guava, *Psidium guajava*) when
406 migrating from higher to lower elevation areas (Blake *et al.* 2015). By preferentially feeding on
407 guava in agricultural areas, tortoises translocate guava seeds and nutrients into other habitats
408 during their downslope migration, resulting in the spread of guava as an invasive species and
409 posing a challenge to the maintenance of natural plant communities in Galapagos National Park
410 (Ellis-Soto *et al.* 2017). The distribution of guava has been mapped through local vegetation
411 sampling plots and drone and remote sensing imagery (Rivas-Torres *et al.* 2018; Laso *et al.*
412 2019). Coupling tortoise movement patterns, resource selection, and habitat structure makes it
413 possible to quantify giant tortoise vectored nutrient transfer in Santa Cruz Island, Galapagos.

414 Santa Cruz Island shows a distinct zonation of vegetation. Dry xerothermic plants dominate the
415 low elevations of the national park, with rainfall and the presence of introduced species (e.g.,
416 guava) increasing with elevation (Itow 2003). During their downslope migration, adult tortoises
417 can migrate from agricultural areas at higher elevations into the lowlands of the Galapagos
418 National Park (identified through net square displacement, Suppl. Material 1). Overlapping
419 home ranges (Winner *et al.* 2018) of tagged tortoises located in the lowlands inside the national
420 park can reveal core areas of tortoise utilization distributions, providing a picture of spatial
421 trophic structure. Using this core area, a stratified sampling of surrounding vegetation, soil
422 samples, and description of microtopography can help understand nutrient composition,
423 microbial activity and abiotic properties of selected areas in an attempt to further characterize
424 habitat structure. Such measurements could be compared with samples obtained in areas
425 where tortoises are absent, serving as a control plot (i.e. via exclosures or randomly selecting
426 points outside the tortoise core area) to further isolate animal impacts on biogeochemical cycles
427 and ecosystem fluxes.

428 Given their different photosynthetic pathways (C3 and CAM, respectively) guava likely contains
429 a different isotopic signature (Sage & Zhu 2011) than the tortoises' most-consumed xerothermic
430 plant at lower elevations of the National Park, the *Opuntia echios* cacti. Thus, stable isotope
431 analysis of fecal matter containing guava could disentangle contributions by tortoises during
432 their migrations from a donor ecosystem (agricultural areas) to a recipient ecosystem (lowlands
433 of the Galapagos National Park) and make spatially explicit predictions of this animal-vectored
434 nutrient flux. Finally, all of these measures can be combined to develop a nutrient budget for the
435 lowland ecosystem of the Galapagos National Park and include the downslope migration of *C.*
436 *porteri* as the mechanism for vectored subsidy (Fig. 3, Fig. 4). Such nutrient ecosystem budgets
437 often attempt to quantify the flows of nutrients through different pools providing an
438 understanding of how these flows may impact ecosystem functioning (Loreau & Holt 2004).
439 Coupling an assessment of nutrient loading with past and present tortoise population numbers
440 could provide a baseline for ongoing conservation initiatives aimed at restoring degraded island
441 habitats by reintroducing giant tortoises to act as ecosystem engineers (Gibbs *et al.* 2010;
442 Hunter *et al.* 2020). We provide the necessary code to replicate steps detailed in this conceptual
443 tortoise example (Suppl. Material 1).

444 **Quantifying how *Canis lupus* creates landscape heterogeneity through prey hunting and**
445 **killing**

446

447 Predators can have profound cascading impacts on ecosystem nutrient dynamics mediated by
448 their effects on prey mortality and space use (Fig. 5). For example, the hunting behaviour of
449 wolves (*Canis lupus*) and the subsequent deposition of prey carcasses may create nutrient
450 hotspots across a landscape, creating heterogeneity in nutrient distribution as carcasses
451 decompose at sites with high rates of predation (Bump *et al.* 2009a; Joseph *et al.* 2009). To
452 explore this, a recursive analysis (Bracis *et al.* 2018) based on how often animals return to
453 specific landscape areas defined by a determined circular radii — which could be chosen based
454 on grain sizes identified from First Passage Times (Mertes *et al.* 2020) — display where and
455 how collared wolves revisit areas in their range. Coupling accelerometer and animal location
456 data can identify hunting, eating, and killing by predators in the wild through behavioural
457 classification and ground-truthing GPS clusters at presumed kill sites (Williams *et al.* 2014;
458 Wang *et al.* 2015). These methodologies can pinpoint the exact coordinates and time of hunting
459 and killing events and therefore quantify the movement of the nutrients through these
460 processes. Once a carcass's presence is identified, camera traps can provide insight into how
461 the predation behaviours of top predators may have cascading impacts on subsidizing
462 scavengers and invertebrates (Perrig *et al.* 2017; Cunningham *et al.* 2018).

463
464 Using a stratified sampling scheme of plant and soil characteristics, it is also possible to quantify
465 the nutrients deposited by the carcasses, explore the spatial diffusion of those nutrients, and
466 estimate how long those nutrients stay in the local system before leaching away or being
467 scavenged. These sites can be compared to measurements collected in randomly selected
468 points, which may serve as a control treatment. Assessing the plant community composition and
469 cover will help identify whether killing behaviour of predators leads to changes in plant
470 composition, while soil samples collected below carcasses can be used to compare microbial
471 activity and nutrient availability between carcass and control sites (Metcalf *et al.* 2016; Risch *et al.*
472 *et al.* 2020). Both total soil and plant nutrient concentration as well as enriched $\delta^{15}\text{N}$ in plant and
473 soil samples can be used to identify and quantify the impact of this animal vectorized subsidy
474 (Bump *et al.* 2009b; Holtgrieve *et al.* 2009; Barton *et al.* 2016). This conceptual study design
475 highlights how predators could concentrate nutrients at kill sites, contributing to landscape
476 heterogeneity with potential knock-on effects on scavenger and plant community distribution.
477 Such knowledge is key for understanding the ecosystem consequences of predator loss (Ripple
478 *et al.* 2014).

479

480 **Moving forward: Future Directions**

481
482 We have illustrated how individual studies may productively integrate disparate fields and tools
483 to address specific questions about animal-vectorized nutrient subsidies within a study system.
484 These disciplines and methodologies can be united to address larger questions about animals
485 and nutrient transport in diverse systems and at multiple scales. Below, we identify the next
486 frontiers in ecological research, which can be resolved through synergistic research linking
487 animal movement and nutrient transport.

488

489 **Improve tracing and mapping of animal vectorized subsidies**

490

491 We see opportunities to improve predictions of animal vectored subsidies based on advances of
492 Species Distribution Modeling (SDM) such as incorporating a priori expert knowledge (Merow *et*
493 *al.* 2016) and joint species distribution modeling (jSDM) (Pollock *et al.* 2014). Such expert
494 knowledge can represent species geographic ranges or species specific elevational ranges as
495 known from field guides. Expert knowledge could enter StDM's in the form of a statistical offset
496 which has been shown to improve model predictions from SDM's (Ellis-Soto *et al.* n.d.; Merow
497 *et al.* 2016). Such offset is independent of the predictor variable (nutrient quantity or quality) and
498 would provide *a priori* expectations of how resources are distributed across a study region
499 rather than assuming an equal likelihood for each cell in a landscape. StDMs could also
500 incorporate soil nutrient maps derived from coarse scale remote sensing (soilgrids database) as
501 an offset reflecting the a priori expectation of a nutrient concentration in a cell. We refer to
502 Merow, Wilson, & Jetz, (2017) for specifics about deploying offsets in logistic regression, but the
503 motivation is that expert information can provide estimates that are complementary to point
504 estimates that could predict nutrient quantity (g/m^2) or nutrient ratios (C:N).

505

506 jSDMs predict spatial occurrences of entire communities of species, rather than distributions of
507 single species, as in SDM (Pollock *et al.* 2014). StDMs could be similarly extended to consider
508 the distribution of multiple individual nutrients (not just their ratios). Particularly, we see potential
509 in adapting jSDM developments from Generalized joint attribute modelling (Clark *et al.* 2017),
510 Bayesian Ordination and Regression Analysis of Multivariate Abundance Data (Hui 2016), and
511 Spatial factor analysis (Thorson *et al.* 2015) to develop joint StDM. Such jStDM could be
512 overlapped with autocorrelated kernel density estimators (Fleming *et al.* 2015) to investigate
513 how animal space use relates to spatial stoichiometry.

514

515 We see potential in building upon mechanistic models of animal movement and seed and
516 nutrient dispersal to map the distribution and magnitude of animal vectored subsidies (Bampoh
517 *et al.* 2019; Kleyheeg *et al.* 2019; van Toor *et al.* 2019). These models couple animal movement
518 and gut retention with remotely sensed land cover information to create spatially explicit maps of
519 nutrient dispersal. Such models have provided insights about how extinct and extant animals
520 have influenced nutrient translocations at coarse spatial scales across the globe (Doughty *et al.*
521 2016; Doughty 2017). These estimates could be refined by incorporating movement models
522 such as allometric random walks (Hirt *et al.* 2018) and individual based movement models
523 (Bampoh *et al.* 2019), rather than coarser lateral diffusion movement models which have
524 hitherto been used.

525

526 **Estimating animal-mediated nutrient translocation within a home range**

527

528 Core areas where individuals within groups or populations might have strongest animal-
529 vectorized subsidies effects can be identified using home range overlap indices between
530 individuals. Such overlap indices may be simple convex hulls around individual home ranges to
531 describe population ranges or more sophisticated utilization distributions based on bias-
532 corrected Bhattacharyya coefficient as shown by Winner *et al.*, (2018). RSFs of individuals with
533 overlapping home ranges could reflect how these animals utilize resources across long-term
534 timescales.

535

536 Behavioural pattern identification could characterize a suite of animal behaviours within home
537 ranges (e.g., forage, rest, fight, prey capture; Kie *et al.* 2010) to identify how animals transport
538 nutrients at shorter timescales (Fig. 3). Revisitation and accelerometer analysis hold promise to
539 identify feeding sites, scent marking sites or latrines (Bracis *et al.* 2018; Bidder *et al.* 2020). High
540 urine concentration at latrines could influence plant communities, soil nutrient loads, and
541 microbial communities, constituting a nutrient hotspot. Other methods estimate nest locations
542 and reproductive output from telemetry data (Picardi *et al.* 2019; Bidder *et al.* 2020). Such
543 behavioural identification can identify where animals assimilate or excrete resources and under
544 which conditions animals act as nutrient sources (bring more nutrients in than they consume,
545 i.e. high urine concentration at latrines or high offspring mortality at nests) or sinks (have a
546 negative net effect on nutrient concentrations at the site). Calculating integrated step selection
547 functions (Avgar *et al.* 2016) using exclusively animal locations that were associated with
548 foraging behaviour (Nathan *et al.* 2012) could identify such nutrient sources. Habitat selection

549 could be explored at fine detail by using drones to create study-site specific landcover maps
550 (Strandburg-Peshkin *et al.* 2017).

551

552 **Animal-vectored subsidies in the Anthropocene**

553

554 In human-modified landscapes, animals find themselves crossing a matrix of fragmented
555 habitats and human pressures (i.e. population density, infrastructure and agricultural areas) that
556 vary in permeability. Human modification of landscapes, such as urban development of roads or
557 C4 plant monocultures for agriculture, can alter diet and nutrient transfer by animals (Magioli *et*
558 *al.* 2019). For example, Roe deer (*Capreolus capreolus*) in central France routinely act as
559 vectors for large quantities of artificially-introduced nitrogen, which they obtain by foraging in
560 agricultural areas, which are deposited near resting sites in forested areas (Abbas *et al.* 2012).
561 In New Mexico, USA, snow geese (*Chen caerulescens*) perform daily foraging trips from wildlife
562 refuges to agricultural areas to feed on corn and alfalfa. This nutrient translocation was shown
563 to increase phosphorous nutrient loadings up to 75% in wetland ponds (Kitchell *et al.* 1999).
564 Thus, animals can link natural areas with human modified landscapes and modify the nutrient
565 budgets of ecosystems.

566 Mechanistic models of animal vectored subsidies (Bampoh *et al.* 2019) could predict
567 how nutrient budgets of ecosystems are altered by the removal of species, such as large bodied
568 animals (Bello *et al.* 2015; Sobral *et al.* 2017), or specific individuals (i.e. elephant bulls in
569 Kruger National Park (Davies & Asner 2019)), or animal introductions (goat introduction in the
570 Galapagos (Bastille-Rousseau *et al.* 2017)). These models could identify causal links between
571 ecosystem functioning and animal mediated subsidies. Such knowledge would provide evidence
572 to rewilding initiatives aiming to restore lost ecosystem services through animal reintroductions
573 (Falcon Wilfredo & Hansen 2018; Lundgren *et al.* 2018).

574

575 **Conclusion**

576

577 Understanding how animals move through both natural and human dominated landscapes to
578 influence ecosystem properties and functions is in need of concerted analysis. To this end, we
579 have provided a methodological road map that draws together methods of analysis across
580 disciplinary fields. We show how, when combined, these can lead to integrative, coherent
581 understanding of how animal vectored subsidies drive spatial ecosystem structure and
582 functioning. It is through the integration and collaboration of disciplines that we can address and

583 understand the importance of this type of nutrient transport in a spatially explicit manner. We
584 hope that the introduced methodological roadmap will facilitate empirical studies that quantify
585 how much the fluxes of nutrients from one pool to another across landscapes can be attributed
586 to animal-vectored subsidies.

587

588 **Acknowledgments:** We thank Kevin Winner, Steven Blake, Brett Jesmer, Ruth Yvonne Oliver
589 and Nathalie Sommers for helpful feedback on this publication. The authors declare no
590 competing interests. This work was supported by a Rufford Small Grant to D.E.S. and a GRFP
591 to K.M.F. under NSF grant no. DGE-1752134. O.J.S. acknowledges funding from the Yale
592 School of the Environment. The authors declare no conflict of interest. All authors conceived the
593 ideas and designed methodology; D.E.S conducted all necessary data analysis; D.E.S and
594 K.M.F. led the writing of the manuscript. D.E.S. and O.J.S. created the figures of the
595 manuscript. All authors contributed to this work and provided final approval for publication.

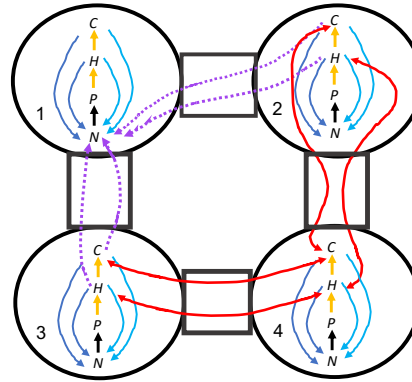
596

$$\frac{dN_i}{dt} = I - EN_i - U(N_i, P_i) + \epsilon M(P_i) + \chi_H L_H(H_i) + \chi_C L_C(C_i) + \gamma_H W(P_i, H_i) + \gamma_C W(H_i, C_i) + d_H \sum_{j=1}^n c_{ij} \gamma_H W(P_j, H_j) + d_C \sum_{j=1}^n c_{ij} \gamma_C W(H_j, C_j)$$

$$\frac{dP_i}{dt} = U(N_i, P_i) - M(P_i) - W(P_i, H_i)$$

$$\frac{dH_i}{dt} = (1 - \gamma_H) W_H(P_i, H_i) - L_H(H_i) + d_H \sum_{j=1}^n c_{ij} H_j - W_C(H_i, C_i)$$

$$\frac{dC_i}{dt} = (1 - \gamma_C) W_C(H_i, C_i) - L_C(C_i) + d_C \sum_{j=1}^n c_{ij} C_j$$



Ecosystem model component

Spatial measurements needed (sections)

Trophic interactions within and between local ecosystems
Nutrient translocation and deposition due to within-ecosystem carcass and nutrient deposition and between ecosystem nutrient deposition

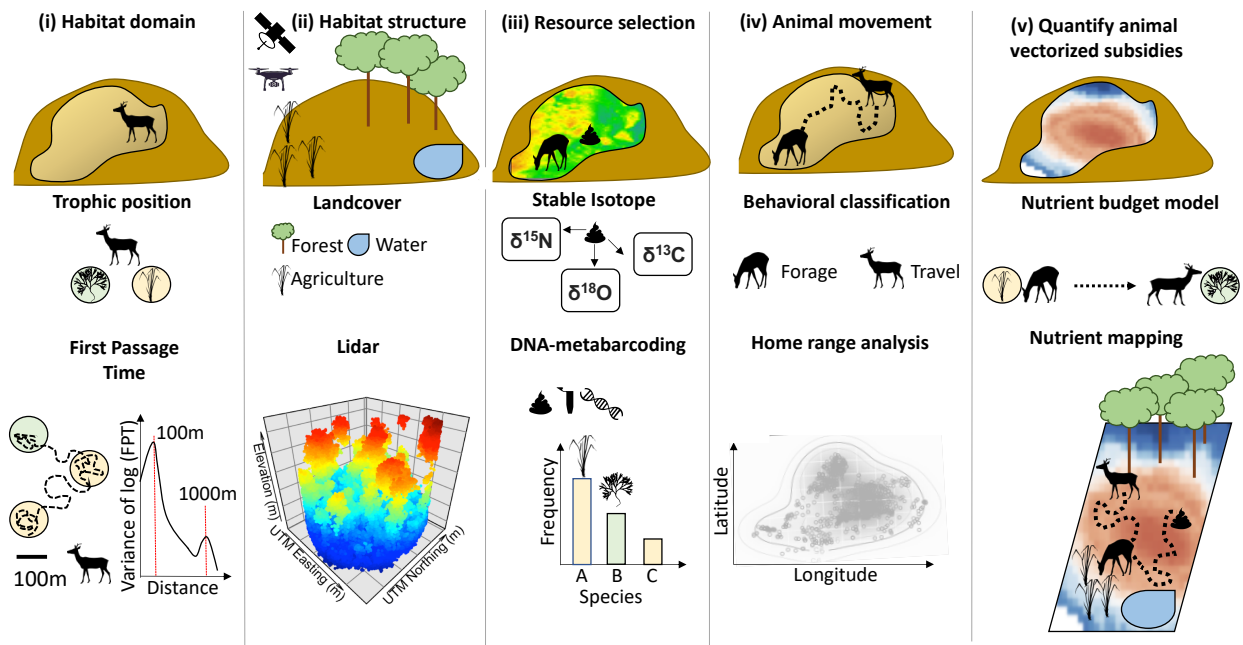
- (i) The spatial extent and spatial grain size of animal movement
- (ii) Habitat structure shaping where animals move
- (iii) Available and selected resources
- (iv) Movement rates directional spatial flow of animals and nutrients
- (v) Amount of animal carcass and nutrients deposited spatially

599

600 **Figure 1:** Meta-ecosystem model characterizing the trophic structure and dynamics of nutrients
601 (N), plants (P), herbivores (H) and carnivores (C) within and between four local ecosystems. In
602 the model carnivore abundance changes as a function of assimilated intake of
603 herbivore biomass within ecosystem i $(1 - \gamma_C)W_C(H_i, C_i)$, where γ_C is the degree of inefficiency in
604 assimilation, loss due to natural mortality at rate $L_C(C_i)$, and gain due to
605 migration from another local ecosystem $d_C \sum_{j=1}^n c_{ij} C_j$, where d_C is the movement rate of a
606 carnivore and c_{ij} is the spatial connectivity between two local ecosystems (where high values
607 reflect high connectivity and hence high ease of flow). Herbivore abundance changes as a
608 function of assimilated intake of plant biomass $(1 - \gamma_H)W_H(P_i, H_i)$, loss due to natural mortality at
609 rate $L_H(H_i)$, loss due to predation at rate $W_C(H_i, C_i)$ and gain due to migration from another local
610 ecosystem $d_H \sum_{j=1}^n c_{ij} H_j$. Plant biomass changes as a function of nutrient uptake at rate $U(N_i, P_i)$,
611 loss due to senescence at rate $M(P_i)$ and herbivory at rate $W_H(P_i, H_i)$. Finally nutrient
612 abundance changes due to global inputs I from weathering of parent geological material,
613 release from riverine sediments, wind-born dust, or rain-driven and snowmelt-driven run-
614 off, loss due to leaching out of the ecosystem EN_i and plant uptake at rate $U(N_i, P_i)$, and

615 additions due to recycling of plant material $\epsilon M(P_i)$, herbivore and carnivore carcasses at
 616 rates $\chi_H L_H(H_i) + \chi_C L_C(C_i)$, and release of unassimilated consumption by herbivores and
 617 carnivores (e.g. egesta) at rates $\gamma HW(P_i, H_i) + \gamma CW(H_i, C_i)$. Local ecosystem nutrient budgets
 618 are also subsidized by unassimilated nutrient release as herbivores and carnivores migrate
 619 among local ecosystems $d_H \sum_{(j=1)} c_{ij} \gamma_H W P_j, H_j) + d_C \sum_{(j=1)} c_{ij} \gamma_C W(H_j, C_j)$. These components
 620 describing nutrient dynamics can ultimately be grouped according to two broad spatial
 621 processes: spatial trophic interactions and spatial nutrient translocation and deposition. These
 622 spatial processes can be further decomposed into five subprocesses that require different
 623 methodologies to measure. A coherent picture of spatial nutrient dynamics can be developed
 624 when data from the five subprocess measurements are combined into a dynamic map that
 625 portrays spatial animal movement and nutrient flow in relation to the biophysical features within
 626 and between local ecosystems across a landscape. Model and illustration adapted from
 627 Marleau et al. (2014).

628

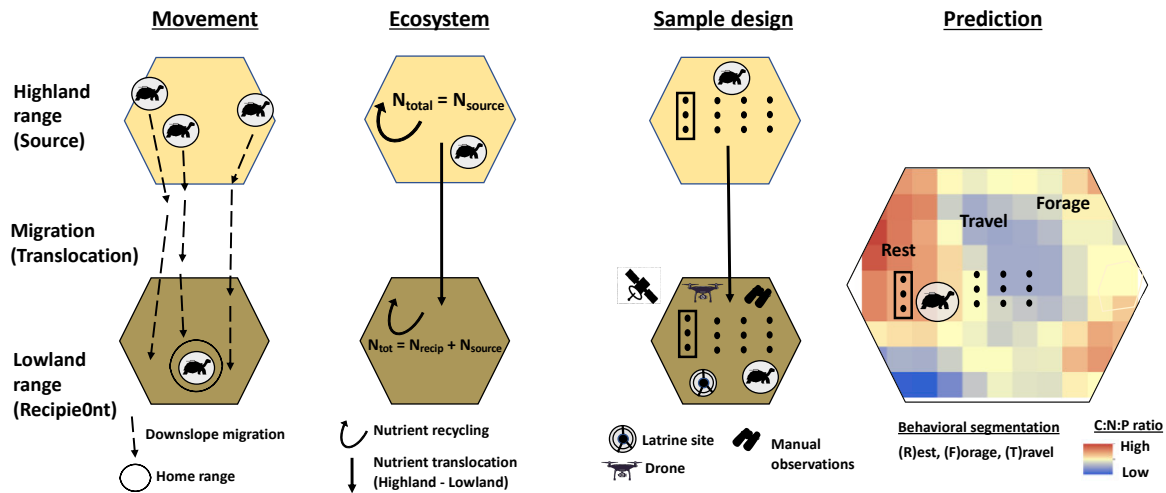


629

630 **Figure 2:** Conceptual demonstration of integrating different disciplines (sections 1,-4) for
 631 quantifying animal vectorized subsidies across a landscape (section 5). (i) The habitat domain
 632 helps understand the trophic position. In our hypothetical example, a roe deer (*Capreolus*
 633 *capreolus*) travels across yellow patches containing agricultural areas and a green patch with
 634 forested area. A first passage time analysis would reveal the scale of roe deer selection to be

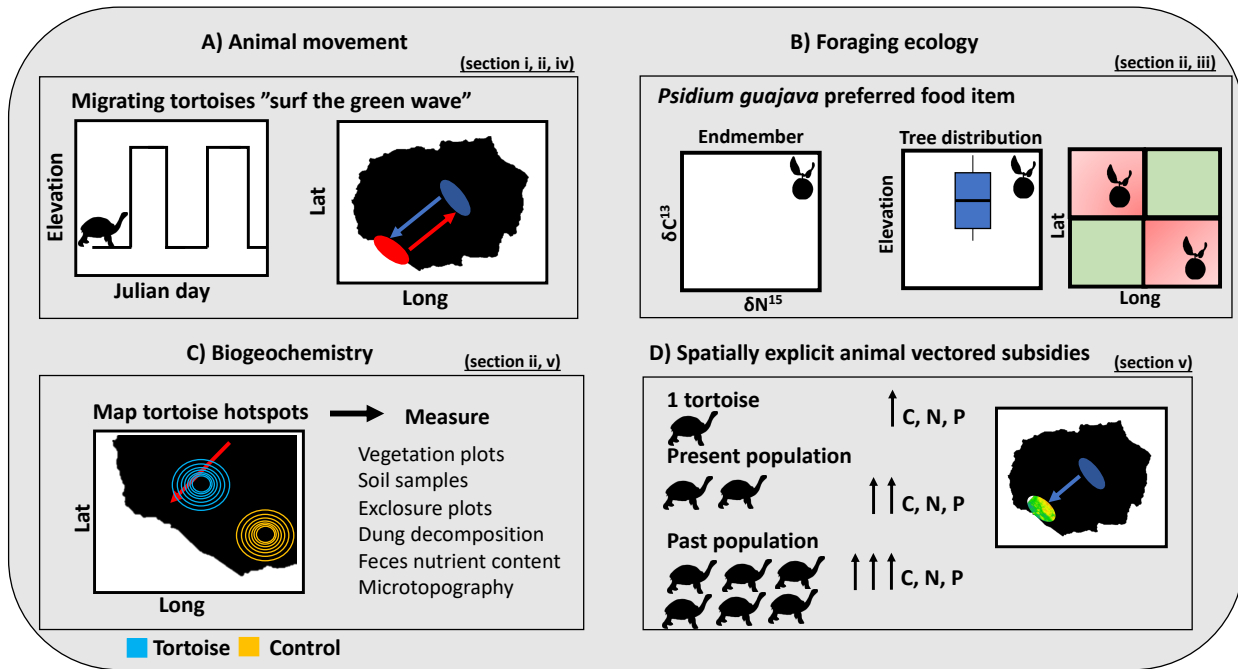
635 strongest at approximately 100m. With this knowledge we can proceed on estimating the trophic
636 positions and interactions at that scale, choosing subsequent remote sensing products at the
637 same spatial scale. If we were to select a scale of 1000m – where extensive remote sensing
638 products are available (Table 1), we would see a weaker response of animals selecting their
639 environment. (ii) The habitat structure of our study region can be identified through remotely
640 sensed products, such as landcover maps. In this example, agriculture and water would be
641 convex ecosystems and likely receive abiotic inputs from forest leaves (concave ecosystem)
642 due to runoff. Convex and concave can be defined with elevation products or with Lidar to
643 obtain a 3D matrix of the environment across which animals navigate (i.e. against elevation
644 gradients during animal upslope movement). Lidar imagery was created using the rLidar and
645 rGedi packages. Habitat and environmental information (ii) can then be used as response
646 variables to understand how animals select and avoid resources and associated habitat
647 structures, using resource selection. Such resource use map is displayed in (iii) with green
648 colors indicating hotspots of habitat selection by our animal. Further, DNA-metabarcoding (iii) of
649 animal fecal matter in the study region can reveal the trophic position and the resources
650 consumed and deposited at great taxonomic detail. Understanding the stoichiometry of
651 resources consumed through stable isotopes (iii) provides insights into the composition and type
652 of nutrients that are moved by animals. (iv) Detailed information of roe deer movement obtained
653 through GPS collars reveals detailed space use of individuals (i.e. their home range) which can
654 be overlaid with the habitat structure of the landscape. Behavioural change point analysis (iv)
655 based on movement data could classify animal behaviour into foraging and travel. Coupling
656 behavioural classification and animal movement with faecal sampling for DNA-metabarcoding
657 and stable isotope can reveal sources (foraging locations) and sinks (excretion locations) of roe
658 deer-vectorized subsidies. (v) Integrating the different methodologies described, allows
659 quantifying animal-vectorized subsidies through spatial modelling such as Stoichiometric
660 Distribution Models (section v; Leroux et al. 2017). Importantly, coupling such models with
661 abiotic nutrient deposition rates (e. g. leaching), allows us to contextualize the magnitude and
662 direction of biotic nutrient deposition rates. We could thus begin including animal vectorized
663 subsidies into ecosystem nutrient budget models (in our hypothetical case the roe deer brings
664 nutrients from the agricultural matrix into the forest ecosystem). Integrating these steps (i-v)
665 allows us to paint a picture of the landscape in which the ecological consequences of moving
666 animals are incorporated into cross-ecosystem models. Silhouettes were obtained from the
667 PhyloPic website (phylopic.org).

668



669
 670 **Figure 3:** Integration of diverse disciplines and methodologies to characterize animal-vectorated
 671 subsidies; in this case nitrogen recycling and translocation by Galapagos tortoises (*Chelonoidis*
 672 *porteri*) in time and space. (a) Movement determines the timing and direction of animal arrival
 673 and departure of ecosystems. (b) Ecosystem nutrient budgets incorporate inputs from outside
 674 ecosystem boundaries, such as animal-vectorated subsidies. (c) Careful sample design helps
 675 elucidating drivers and predict consequences of nutrient transport by animals. Coupling large
 676 extent (remote sensing, drones) with local field measurements (manual, drones) and animal
 677 population estimates, allows (d) quantifying magnitude and flow of animal-vectorated subsidies
 678 in a spatially explicit manner and estimate what proportion of total nutrients are being mobilized
 679 by animals on the move. Tortoise silhouettes were obtained from the PhyloPic website
 680 (phylopic.org).
 681

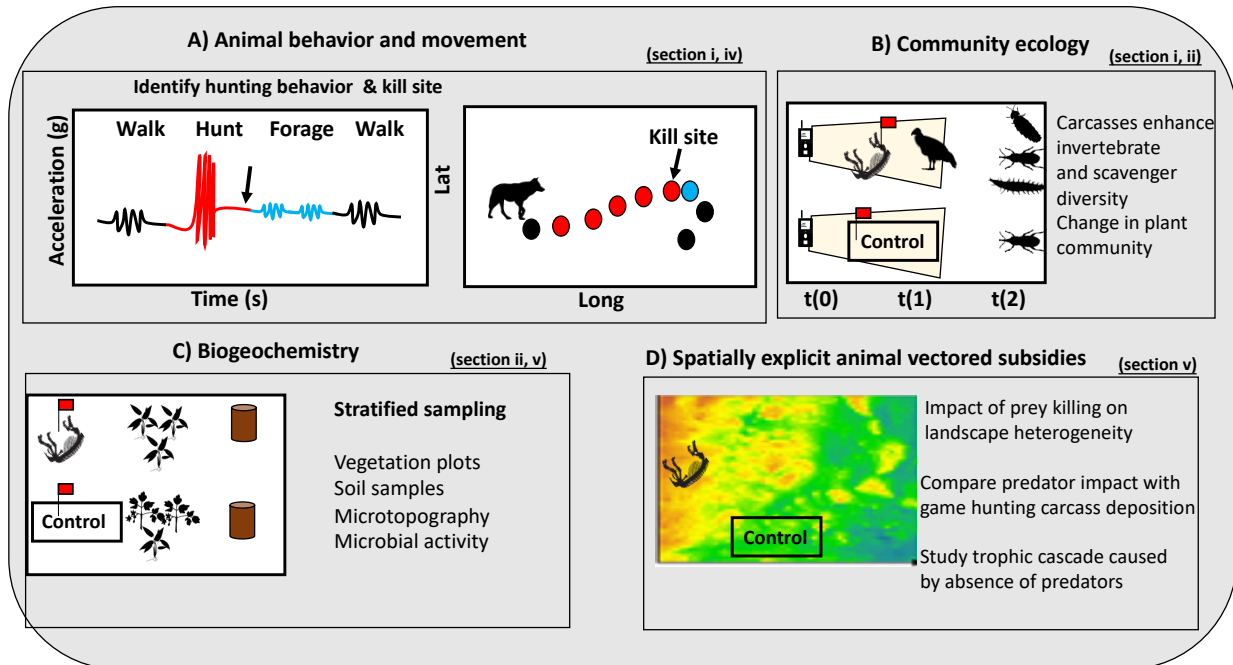
Galapagos tortoise (*Chelonoidis porteri*)



682
 683
 684
 685
 686
 687
 688
 689

Figure 4: Conceptual example of studying nutrient transport of giant tortoises (*Chelonoidis porteri*) in Santa Cruz Island. Integrating known movement patterns and foraging behaviour of this species with the distribution and nutritional composition of food items, it is possible to design an experiment to estimate the influence of tortoises transporting nutrients to the Galapagos National Park boundaries during their downslope migration. Silhouettes were obtained from the PhyloPic website (phylopic.org).

Wolf (*Canis lupus*)



690
 691 **Figure 5:** Conceptual example to identify killing sites of Wolves (*Canis lupus*) with biologging
 692 technologies and quantify how predators drive landscape heterogeneity. Identifying kill sites
 693 allows studying how carcass presence affects local biogeochemistry and community
 694 composition when compared to control locations. Silhouettes were obtained from the PhyloPic
 695 website (phylopic.org).

696
 697 **Table 1:** Collection of applicable remote sensing products for animal mediated subsidies. We
 698 elucidate the spatio-temporal resolution and grain size of these products.

699
 700 **Appendix – Supplementary Material**
 701

702 **Supplementary Material 1: Necessary code to perform movement ecology and remote**
 703 **sensing analysis of the Galapagos tortoise example**

704
 705 **References**

706
 707 Abbas, F., Merlet, J., Morellet, N., Verheyden, H., Hewison, A.J.M., Cargnelutti, B., *et al.* (2012).
 708 Roe deer may markedly alter forest nitrogen and phosphorus budgets across Europe, 1–8.
 709 Allan, B.M., Nimmo, D.G., Ierodiaconou, D., VanDerWal, J., Koh, L.P. & Ritchie, E.G. (2018).
 710 Futurecasting ecological research: the rise of technoecology. *Ecosphere*.

711 Allen, C.D. & Wesner, S.J. (2016). Synthesis: comparing effects of resource and consumer
712 fluxes into recipient food webs using meta- analysis. *Ecology*, 97, 594–604.

713 Amatulli, G., Domisch, S., Tuanmu, M.-N., Parmentier, B., Ranipeta, A., Malczyk, J., *et al.*
714 (2018). A suite of global, cross-scale topographic variables for environmental and
715 biodiversity modeling. *Sci. Data*, 5, 180040.

716 de Araujo Barbosa, C.C., Atkinson, P.M. & Dearing, J.A. (2015). Remote sensing of ecosystem
717 services: A systematic review. *Ecol. Indic.*, 52, 430–443.

718 Atkins, J.L., Long, R.A., Pansu, J., Daskin, J.H., Potter, A.B., Stalmans, M.E., *et al.* (2019).
719 Cascading impacts of large-carnivore extirpation in an African ecosystem. *Science (80-.)*,
720 364, 173–177.

721 Atkinson, C.L., Capps, K.A., Rugenski, A.T. & Vanni, M.J. (2017). Consumer-driven nutrient
722 dynamics in freshwater ecosystems : from individuals to ecosystems. *Biol. Rev.*, 92, 2003–
723 2023.

724 Avgar, T., Potts, J.R., Lewis, M.A. & Boyce, M.S. (2016). Integrated step selection analysis:
725 bridging the gap between resource selection and animal movement. *Methods Ecol. Evol.*,
726 7, 619–630.

727 Bampoh, D., Earl, J.E. & Zollner, P.A. (2019). Examining the relative influence of animal
728 movement patterns and mortality models on the distribution of animal transported
729 subsidies. *Ecol. Modell.*, 412, 108824.

730 Barton, P.S., McIntyre, S., Evans, M.J., Bump, J.K., Cunningham, S.A. & Manning, A.D. (2016).
731 Substantial long-term effects of carcass addition on soil and plants in a grassy eucalypt
732 woodland. *Ecosphere*, 7, e01537.

733 Bastille-Rousseau, G., Gibbs, J.P., Campbell, K., Yackulic, C.B. & Blake, S. (2017). Ecosystem
734 implications of conserving endemic versus eradicating introduced large herbivores in the
735 Galapagos Archipelago. *Biol. Conserv.*, 209, 1–10.

736 Bastille-Rousseau, G., Potts, J.R., Yackulic, C.B., Frair, J.L., Ellington, E.H. & Blake, S. (2016).
737 Flexible characterization of animal movement pattern using net squared displacement and
738 a latent state model. *Mov. Ecol.*, 4, 15.

739 Bastille-Rousseau, G., Yackulic, C., Gibbs, J., Frair, J., Cabrera, F. & Blake, S. (2019).
740 Migration triggers in a large herbivore: Galapagos giant tortoises navigating resource
741 gradients on volcanoes. *Ecology*, 100, 1–11.

742 Bauer, S. & Hoyer, B.J. (2014). Migratory animals couple biodiversity and ecosystem functioning
743 worldwide. *Science (80-.)*, 344.

744 Bello, C., Galetti, M., Pizo, M.A., Magnago, L.F.S., Rocha, M.F., Lima, R.A.F., *et al.* (2015).

745 Defaunation affects carbon storage in tropical forests. *Sci. Adv.*, 1, e1501105.

746 Ben-David, M. & Flaherty, E.A. (2012). Stable isotopes in mammalian research: a beginner's
747 guide. *J. Mammal.*, 93, 312–328.

748 Bennison, A., Bearhop, S., Bodey, T.W., Votier, S.C., Grecian, W.J., Wakefield, E.D., *et al.*
749 (2018). Search and foraging behaviors from movement data: A comparison of methods.
750 *Ecol. Evol.*, 8, 13–24.

751 Bergen, K.M., Goetz, S.J., Dubayah, R.O., Henebry, G.M., Hunsaker, C.T., Imhoff, M.L., *et al.*
752 (2009). Remote sensing of vegetation 3-D structure for biodiversity and habitat: Review
753 and implications for lidar and radar spaceborne missions. *J. Geophys. Res.*
754 *Biogeosciences*, 114, G00E06.

755 Berzaghi, F., Verbeeck, H., Nielsen, M.R., Doughty, C.E., Bretagnolle, F., Marchetti, M., *et al.*
756 (2018). Assessing the role of megafauna in tropical forest ecosystems and biogeochemical
757 cycles - the potential of vegetation models. *Ecography (Cop.)*, 1934–1954.

758 Bidder, O.R., di Virgilio, A., Hunter, J.S., McInturff, A., Gaynor, K.M., Smith, A.M., *et al.* (2020).
759 Monitoring canid scent marking in space and time using a biologging and machine learning
760 approach. *Sci. Rep.*, 10, 588.

761 Blake, S., Guézou, A., Deem, S.L., Yackulic, C.B. & Cabrera, F. (2015). The Dominance of
762 Introduced Plant Species in the Diets of Migratory Galapagos Tortoises Increases with
763 Elevation on a Human-Occupied Island. *Biotropica*, 47, 246–258.

764 Blake, S., Wikelski, M., Cabrera, F., Guezou, A., Silva, M., Sadeghayobi, E., *et al.* (2012). Seed
765 dispersal by Galapagos tortoises. *J. Biogeogr.*, 39, 1961–1972.

766 Boyce, M.S., Vernier, P.R., Nielsen, S.E. & Schmiegelow, F.K.A. (2002). Evaluating resource
767 selection functions. *Ecol. Modell.*, 281–300.

768 Bracis, C., Bildstein, K.L. & Mueller, T. (2018). Revisitation analysis uncovers spatio-temporal
769 patterns in animal movement data. *Ecography (Cop.)*, 41, 1801–1811.

770 Brown, D.D., Kays, R., Wikelski, M., Wilson, R. & Klimley, A.P. (2013). Observing the
771 unwatchable through acceleration logging of animal behavior. *Anim. Biotelemetry*, 1, 1–20.

772 Bump, J.K., Webster, C.R., Vucetich, J.A., Peterson, R.O., Shields, J.M. & Powers, M.D.
773 (2009a). Ungulate Carcasses Perforate Ecological Filters and Create Biogeochemical
774 Hotspots in Forest Herbaceous Layers Allowing Trees a Competitive Advantage.
775 *Ecosystems*, 12, 996–1007.

776 Bump, K.J., Rolf, O.P. & Vucetich, A.J. (2009b). Wolves modulate soil nutrient heterogeneity
777 and foliar nitrogen by configuring the distribution of ungulate carcasses. *Ecology*, 90,
778 3159–3167.

779 Chapin, F.S., Matson, P.A. & Vitousek, P.M. (2012). *Principles of terrestrial ecosystem ecology*.
780 *Princ. Terr. Ecosyst. Ecol.* Springer.

781 Cherif, M. & Loreau, M. (2013). Plant-herbivore-decomposer stoichiometric mismatches and
782 nutrient cycling in ecosystems. *Proc. R. Soc. B Biol. Sci.*, 280, 20122453.

783 Clark, B.L., Bevanda, M., Aspillaga, E. & Jørgensen, N.H. (2016). Bridging disciplines with
784 training in remote sensing for animal movement: an attendee perspective. *Remote Sens.*
785 *Ecol. Conserv.*, 3, 30–37.

786 Clark, J.S., Nemergut, D., Seyednasrollah, B., Turner, P.J. & Zhang, S. (2017). Generalized
787 joint attribute modeling for biodiversity analysis: median-zero, multivariate, multifarious
788 data. *Ecol. Monogr.*, 87, 34–56.

789 Cunningham, C.X., Johnson, C.N., Barmuta, L.A., Hollings, T., Woehler, E.J. & Jones, M.E.
790 (2018). Top carnivore decline has cascading effects on scavengers and carrion
791 persistence. *Proc. R. Soc. B Biol. Sci.*, 285, 20181582.

792 Davies, A.B. & Asner, G.P. (2019). Elephants limit aboveground carbon gains in African
793 savannas. *Glob. Chang. Biol.*, 25, 1368–1382.

794 Deagle, B.E., Thomas, A.C., McInnes, J.C., Clarke, L.J., Vesterinen, E.J., Clare, E.L., *et al.*
795 (2019). Counting with DNA in metabarcoding studies: How should we convert sequence
796 reads to dietary data? *Mol. Ecol.*, 28, 391–406.

797 Dechmann, D.K.N., Wikelski, M., Ellis-Soto, D., Safi, K. & Teague O'Mara, M. (2017).
798 Determinants of spring migration departure decision in a bat. *Biol. Lett.*

799 Dirzo, R., Young, H.S., Galetti, M., Ceballos, G., Isaac, N.J.B. & Collen, B. (2014). Defaunation
800 in the Anthropocene. *Science (80-)*.

801 Doughty, C.E. (2017). Herbivores increase the global availability of nutrients over millions of
802 years. *Nat. Ecol. Evol.*, 1, 1820–1827.

803 Doughty, C.E., Roman, J., Faurby, S., Wolf, A., Haque, A., Bakker, E.S., *et al.* (2016). Global
804 nutrient transport in a world of giants. *Proc. Natl. Acad. Sci. U. S. A.*, 113, 868–73.

805 Durán, S.M., Martin, R.E., Díaz, S., Maitner, B.S., Malhi, Y., Salinas, N., *et al.* (2019). Informing
806 trait-based ecology by assessing remotely sensed functional diversity across a broad
807 tropical temperature gradient. *Sci. Adv.*, 5, eaaw8114.

808 Earl, J.E. & Zollner, P.A. (2017). Advancing research on animal-transported subsidies by
809 integrating animal movement and ecosystem modelling. *J. Anim. Ecol.*, 86, 987–997.

810 Edelhoff, H., Signer, J. & Balkenhol, N. (2016). Path segmentation for beginners: An overview of
811 current methods for detecting changes in animal movement patterns. *Mov. Ecol.*, 4.

812 Ellis-Felege, S.N., Burnam, J.S., Palmer, W.E., Sisson, D.C., Wellendorf, S.D., Thornton, R.P.,

813 *et al.* (2008). Cameras Identify White-tailed Deer Depredating Northern Bobwhite Nests.
814 *Southeast. Nat.*, 7, 562–564.

815 Ellis-Soto, D., Blake, S., Soutlan, A., Guézou, A., Cabrera, F. & Lötters, S. (2017). Plant species
816 dispersed by Galapagos tortoises surf the wave of habitat suitability under anthropogenic
817 climate change. *PLoS One*, 12, e0181333.

818 Ellis-Soto, D., Merow, C., Amatulli, G., Parra, J.L. & Jetz, W. (n.d.). Continental-scale 1km
819 hummingbird diversity derived from fusing point records with lateral and elevational expert
820 information. *Ecography (Cop.)*, in review.

821 Ellis Soto, D. (2020). Giant tortoises connecting terrestrial and freshwater ecosystems in Santa
822 Cruz Island. In: *Galapagos Giant Tortoises* (eds. Gibbs, J.P., Cayot, L.J. & Tapia, W.).
823 Elsevier, Amsterdam, p. 286.

824 Falcon Wilfredo & Hansen, D.M. (2018). Island rewilding with giant tortoises in an era of climate
825 change.

826 Fauchald, P. & Tveraa, T. (2003). USING FIRST-PASSAGE TIME IN THE ANALYSIS OF
827 AREA-RESTRICTED SEARCH AND HABITAT SELECTION. *Ecology*, 84, 282–288.

828 Fleming, C.H., Fagan, W.F., Mueller, T., Olson, K.A., Leimgruber, P. & Calabrese, J.M. (2015).
829 Rigorous home range estimation with movement data: a new autocorrelated kernel density
830 estimator. *Ecology*, 96, 1182–1188.

831 Fortin, D., Beyer, H.L., Boyce, M.S., Smith, D.W., Duchesne, T. & Mao, J.S. (2005). Wolves
832 influence elk movements: Behavior shapes a trophic cascade in Yellowstone National
833 Park. *Ecology*.

834 Garriga, J., Palmer, J.R.B., Oltra, A. & Bartumeus, F. (2016). Expectation-Maximization Binary
835 Clustering for Behavioural Annotation. *PLoS One*, 11, e0151984.

836 Gibbs, J.P., Sterling, E.J. & Zabala, F.J. (2010). Giant tortoises as ecological engineers: A long-
837 term quasi-experiment in the Galapagos Islands. *Biotropica*, 42, 208–214.

838 Gounand, I., Harvey, E., Little, C.J. & Altermatt, F. (2018a). Meta-Ecosystems 2.0: Rooting the
839 Theory into the Field. *Trends Ecol. Evol.*, 33, 36–46.

840 Gounand, I., Little, C.J., Harvey, E. & Altermatt, F. (2018b). Cross-ecosystem carbon flows
841 connecting ecosystems worldwide. *Nat. Commun.*, 9, 4825.

842 Hancock, S., Hofton, M., Sun, X., Tang, H., Kellner, J.R., Armston, J., *et al.* (2019). The GEDI
843 simulator: A large-footprint waveform lidar simulator for calibration and validation of
844 spaceborne missions. *Earth Sp. Sci.*, 294–310.

845 Hays, G.C., Bailey, H., Bograd, S.J., Bowen, W.D., Campagna, C., Carmichael, R.H., *et al.*
846 (2019). Translating Marine Animal Tracking Data into Conservation Policy and

847 Management. *Trends Ecol. Evol.*, xx, 1–15.

848 Hirt, M.R., Grimm, V., Li, Y., Rall, B.C., Rosenbaum, B. & Brose, U. (2018). Bridging Scales:
849 Allometric Random Walks Link Movement and Biodiversity Research. *Trends Ecol. Evol.*,
850 33, 701–712.

851 Hobson, K.A., Wassenaar, L.I., Bowen, G.J., Courtiol, A., Trueman, C.N., Voigt, C.C., *et al.*
852 (2019). Chapter 10 - Outlook for Using Stable Isotopes in Animal Migration Studies. In:
853 *Tracking Animal Migration with Stable Isotopes (Second Edition)* (eds. Hobson, K.A. &
854 Wassenaar, L.I.). Academic Press, pp. 237–244.

855 Holtgrieve, G.W., Schindler, D.E. & Jewett, P.K. (2009). Large predators and biogeochemical
856 hotspots: Brown bear (*Ursus arctos*) predation on salmon alters nitrogen cycling in riparian
857 soils. *Ecol. Res.*

858 Hui, F.K.C. (2016). boral – Bayesian Ordination and Regression Analysis of Multivariate
859 Abundance Data in R. *Methods Ecol. Evol.*, 7, 744–750.

860 Hunter, E.A., Gibbs, J.P., Cayot, L.J., Tapia, W., Quinzin, M.C., Miller, J.M., *et al.* (2020).
861 Seeking compromise across competing goals in conservation translocations: The case of
862 the ‘extinct’ Floreana Island Galapagos giant tortoise. *J. Appl. Ecol.*, 57, 136–148.

863 Itow, S. (2003). Zonation Pattern, Succession Process and Invasion by Aliens in Species-poor
864 Insular Vegetation of the Galápagos Islands. *Glob. Environ. Res.*, 7, 39–58.

865 Jetz, W., Cavender-Bares, J., Pavlick, R., Schimel, D., Davis, F.W., Asner, G.P., *et al.* (2016).
866 Monitoring plant functional diversity from space. *Nat. Plants*, 2, 16024.

867 Johnson, D.H. (1980). The comparison of usage and availability measurements for evaluating
868 resource preference. *Ecology*, 61.

869 Joo, R., Boone, M.E., Clay, T.A. & Patrick, S.C. (2019). Navigating through the R packages for
870 movement, 1–29.

871 Joseph, K.B., Rolf, O.P. & John, A.V. (2009). Wolves modulate soil nutrient heterogeneity and
872 foliar nitrogen by configuring the distribution of ungulate carcasses. *Ecology*, 90, 3159–
873 3167.

874 Kartzinel, T.R., Chen, P.A., Coverdale, T.C., Erickson, D.L., Kress, W.J., Kuzmina, M.L., *et al.*
875 (2015). DNA metabarcoding illuminates dietary niche partitioning by African large
876 herbivores. *Proc. Natl. Acad. Sci.*, 112, 8019–8024.

877 Kays, R., Crofoot, M.C., Jetz, W. & Wikelski, M. (2015). Terrestrial animal tracking as an eye on
878 life and planet. *Science (80-.)*, 348, aaa2478.

879 Kelson, S.J., Power, M.E., Finlay, J.C. & Carlson, S.M. (2020). Partial migration alters
880 population ecology and food chain length: evidence from a salmonid fish. *Ecosphere*, 11,

881 e03044.

882 Kie, J.G., Matthiopoulos, J., Fieberg, J., Powell, R.A., Cagnacci, F., Mitchell, M.S., *et al.* (2010).
883 The home-range concept: are traditional estimators still relevant with modern telemetry
884 technology? *Philos. Trans. R. Soc. B Biol. Sci.*, 365, 2221–2231.

885 Kitchell, J.F., Schindler, D.E., Herwig, B.R., Post, D.M., Olson, M.H. & Oldham, M. (1999).
886 Nutrient cycling at the landscape scale: The role of diel foraging migrations by geese at the
887 Bosque del Apache National Wildlife Refuge, New Mexico. *Limnol. Oceanogr.*

888 Kleyheeg, E., Fiedler, W., Safi, K., Waldenström, J., Wikelski, M. & van Toor, M.L. (2019). A
889 Comprehensive Model for the Quantitative Estimation of Seed Dispersal by Migratory
890 Mallards. *Front. Ecol. Evol.*, 7, 1–14.

891 Knyazikhin, Y., Schull, M.A., Stenberg, P., Möttus, M., Rautiainen, M., Yang, Y., *et al.* (2013).
892 Hyperspectral remote sensing of foliar nitrogen content. *Proc. Natl. Acad. Sci.*, 110, E185–
893 E192.

894 Kristensen, D.K., Kristensen, E., Forchhammer, M.C., Michelsen, A. & Schmidt, N.M. (2011).
895 Arctic herbivore diet can be inferred from stable carbon and nitrogen isotopes in C3 plants,
896 faeces, and wool. *Can. J. Zool.*, 89, 892–899.

897 Laso, F.J., Ben, L., Rivas-torres, G., Sampedro, C. & Arce-nazario, J. (2019). Land Cover
898 Classification of Complex Agroecosystems in the Non-Protected Highlands of the
899 Galapagos Islands.

900 Leroux, S.J., Hawlena, D. & Schmitz, O.J. (2012). Predation risk, stoichiometric plasticity and
901 ecosystem elemental cycling. *Proc. R. Soc. B Biol. Sci.*, 279, 4183–4191.

902 Leroux, S.J. & Loreau, M. (2008). Subsidy hypothesis and strength of trophic cascades across
903 ecosystems. *Ecol. Lett.*, 11, 1147–1156.

904 Leroux, S.J. & Loreau, M. (2012). Dynamics of Reciprocal Pulsed Subsidies in Local and Meta-
905 Ecosystems. *Ecosystems*, 15, 48–59.

906 Leroux, S.J., Wal, E. Vander, Wiersma, Y.F., Charron, L., Ebel, J.D., Ellis, N.M., *et al.* (2017).
907 Stoichiometric distribution models: ecological stoichiometry at the landscape extent. *Ecol.*
908 *Lett.*, 20, 1495–1506.

909 Lindeman, R.L. (1942). The Trophic-Dynamic Aspect of Ecology. *Ecology*, 23, 399–417.

910 Loreau, M. & Holt, R.D. (2004). Spatial Flows and the Regulation of Ecosystems. *Am. Nat.*, 163,
911 606–615.

912 Loreau, M., Mouquet, N. & Holt, R.D. (2003). IDEAS AND Meta-ecosystems : a theoretical
913 framework for a spatial ecosystem ecology, 673–679.

914 Lundgren, E.J., Ramp, D., Ripple, W.J. & Wallach, A.D. (2018). Introduced megafauna are

915 rewilding the Anthropocene. *Ecography (Cop.)*, 41, 857–866.

916 Maclean, I.M.D. (2020). Predicting future climate at high spatial and temporal resolution. *Glob.*
917 *Chang. Biol.*, 26, 1003–1011.

918 Maclean, I.M.D., Mosedale, J.R. & Bennie, J.J. (2019). Microclima: An r package for modelling
919 meso- and microclimate. *Methods Ecol. Evol.*, 10.

920 Magioli, M., Moreira, M.Z., Fonseca, R.C.B., Ribeiro, M.C., Rodrigues, M.G. & Ferraz, K.M.P.M.
921 de B. (2019). Human-modified landscapes alter mammal resource and habitat use and
922 trophic structure. *Proc. Natl. Acad. Sci.*, 116, 18466–18472.

923 Mahoney, P.J. & Young, J.K. (2017). Uncovering behavioural states from animal activity and
924 site fidelity patterns. *Methods Ecol. Evol.*, 8, 174–183.

925 Marleau, J.N., Guichard, F. & Loreau, M. (2014). Meta-ecosystem dynamics and functioning on
926 finite spatial networks. *Proc. R. Soc. B Biol. Sci.*

927 Massol, F., Gravel, D., Mouquet, N., Cadotte, M.W., Fukami, T. & Leibold, M.A. (2011). Linking
928 community and ecosystem dynamics through spatial ecology. *Ecol. Lett.*, 14, 313–323.

929 McCann, K.S., Rasmussen, J.B. & Umbanhowar, J. (2005). The dynamics of spatially coupled
930 food webs. *Ecol. Lett.*, 8, 513–523.

931 McInturf, A.G., Pollack, L., Yang, L.H. & Spiegel, O. (2019). Vectors with autonomy : what
932 distinguishes animal-mediated nutrient transport from abiotic vectors ?

933 McLean, K.A., Trainor, A.M., Asner, G.P., Crofoot, M.C., Hopkins, M.E., Campbell, C.J., *et al.*
934 (2016). Movement patterns of three arboreal primates in a Neotropical moist forest
935 explained by LiDAR-estimated canopy structure. *Landsc. Ecol.*, 31, 1849–1862.

936 McSherry, M.E. & Ritchie, M.E. (2013). Effects of grazing on grassland soil carbon: a global
937 review. *Glob. Chang. Biol.*, 19, 1347–1357.

938 Merow, C., Allen, J.M., Aiello-Lammens, M. & Silander, J.A. (2016). Improving niche and range
939 estimates with Maxent and point process models by integrating spatially explicit
940 information. *Glob. Ecol. Biogeogr.*, 25, 1022–1036.

941 Merow, C., Wilson, A.M. & Jetz, W. (2017). Integrating occurrence data and expert maps for
942 improved species range predictions. *Glob. Ecol. Biogeogr.*, 26, 243–258.

943 Mertes, K., Jarzyna, M.A. & Jetz, W. (2020). Hierarchical multi-grain models improve
944 descriptions of species' environmental associations, distribution, and abundance. *Ecol.*
945 *Appl.*

946 Mertes, K. & Jetz, W. (2017). Disentangling scale dependencies in species environmental
947 niches and distributions. *Ecography (Cop.)*.

948 Metcalf, J.L., Xu, Z.Z., Weiss, S., Lax, S., Van Treuren, W., Hyde, E.R., *et al.* (2016). Microbial

949 community assembly and metabolic function during mammalian corpse decomposition.
950 *Science* (80-.).

951 Michelot, T. & Blackwell, P.G. (2019). State-switching continuous-time correlated random walks.
952 *Methods Ecol. Evol.*, 0, 1–13.

953 Michelot, T., Blackwell, P.G. & Matthiopoulos, J. (2019). Linking resource selection and step
954 selection models for habitat preferences in animals. *Ecology*, 100, e02452.

955 Montagano, L., Leroux, S.J., Giroux, M.-A. & Lecomte, N. (2019). The strength of ecological
956 subsidies across ecosystems: a latitudinal gradient of direct and indirect impacts on food
957 webs. *Ecol. Lett.*, 22, 265–274.

958 Nathan, R., Getz, W.M., Revilla, E., Holyoak, M., Kadmon, R., Saltz, D., *et al.* (2008). A
959 movement ecology paradigm for unifying organismal movement research. *PNAS*, 105,
960 19052–19059.

961 Nathan, R., Spiegel, O., Fortmann-Roe, S., Harel, R., Wikelski, M. & Getz, W.M. (2012). Using
962 tri-axial acceleration data to identify behavioral modes of free-ranging animals: general
963 concepts and tools illustrated for griffon vultures. *J. Exp. Biol.*, 215, 986–96.

964 Newsome, S.D., Clementz, M.T. & Koch, P.L. (2010). Using stable isotope biogeochemistry to
965 study marine mammal ecology. *Mar. Mammal Sci.*, 26, 509–572.

966 Pansu, J., Guyton, J.A., Potter, A.B., Atkins, J.L., Daskin, J.H., Wursten, B., *et al.* (2019).
967 Trophic ecology of large herbivores in a reassembling African ecosystem. *J. Ecol.*, 107,
968 1355–1376.

969 Patterson, T.A., Thomas, L., Wilcox, C., Ovaskainen, O. & Matthiopoulos, J. (2008).
970 State–space models of individual animal movement. *Trends Ecol. Evol.*, 23, 87–
971 94.

972 Perrig, P.L., Donadio, E., Middleton, A.D. & Pauli, J.N. (2017). Puma predation subsidizes an
973 obligate scavenger in the high Andes. *J. Appl. Ecol.*, 54, 846–853.

974 Pettorelli, N., Laurance, W.F., O'Brien, T.G., Wegmann, M., Nagendra, H. & Turner, W. (2014).
975 Satellite remote sensing for applied ecologists: Opportunities and challenges. *J. Appl.*
976 *Ecol.*, 51, 839–848.

977 Pettorelli, N., to Bühne, H., Tulloch, A., Dubois, G., Macinnis-Ng, C., Queirós, A.M., *et al.*
978 (2018). Satellite remote sensing of ecosystem functions: opportunities, challenges and way
979 forward. *Remote Sens. Ecol. Conserv.*, 4, 71–93.

980 Picardi, S., Smith, B.J., Boone, M.E., Frederick, P.C., Cecere, J.G., Rubolini, D., *et al.* (2019). A
981 data-driven method to locate nest sites and estimate reproductive outcome from avian
982 telemetry data. *bioRxiv*, 562025.

983 Pollock, L.J., Tingley, R., Morris, W.K., Golding, N., O'Hara, R.B., Parris, K.M., *et al.* (2014).
984 Understanding co-occurrence by modelling species simultaneously with a Joint Species
985 Distribution Model (JSDM). *Methods Ecol. Evol.*, 5, 397–406.

986 Post, D.M. (2002). Using stable isotopes to estimate trophic position: Models, methods, and
987 assumptions. *Ecology*.

988 Remelgado, R., Leutner, B., Safi, K., Sonnenschein, R., Kuebert, C. & Wegmann, M. (2017).
989 Linking animal movement and remote sensing - mapping resource suitability from a remote
990 sensing perspective. *Remote Sens. Ecol. Conserv.*, 1–14.

991 Remelgado, R., Wegmann, M. & Safi, K. (2019). rsmove —An r package to bridge remote
992 sensing and movement ecology . *Methods Ecol. Evol.*

993 Ripple, W.J., Estes, J.A., Beschta, R.L., Wilmers, C.C., Ritchie, E.G., Hebblewhite, M., *et al.*
994 (2014). Status and Ecological Effects of the World's Largest Carnivores. *Science (80-.)*,
995 343, 1241484.

996 Risch, A.C., Frossard, A., Schütz, M., Frey, B., Morris, A.W. & Bump, J.K. (2020). Effects of elk
997 and bison carcasses on soil microbial communities and ecosystem functions in
998 Yellowstone, USA. *Funct. Ecol.*, 00, 1–12.

999 Rivas-Torres, G.F., Benítez, F.L., Rueda, D., Sevilla, C. & Mena, C.F. (2018). A methodology
1000 for mapping native and invasive vegetation coverage in archipelagos: An example from the
1001 Galápagos Islands. *Prog. Phys. Geogr.*

1002 Sage, R.F. & Zhu, X.-G. (2011). Exploiting the engine of C(4) photosynthesis. *J. Exp. Bot.*

1003 Schmitz, O.J., Hawlena, D. & Trussell, G.C. (2010). Predator control of ecosystem nutrient
1004 dynamics. *Ecol. Lett.*

1005 Schmitz, O.J., Miller, J.R.B., Trainor, A.M. & Abrahms, B. (2017). Toward a community ecology
1006 of landscapes: predicting multiple predator–prey interactions across geographic space.
1007 *Ecology*, 98, 2281–2292.

1008 Schmitz, O.J., Rosenblatt, A.E. & Smylie, M. (2016). Temperature dependence of predation
1009 stress and the nutritional ecology of a generalist herbivore. *Ecology*, 97, 3119–3130.

1010 Schmitz, O.J., Wilmers, C.C., Leroux, S.J., Doughty, C.E., Atwood, T.B., Galetti, M., *et al.*
1011 (2018). Animals and the zoogeochemistry of the carbon cycle. *Science (80-.)*, 362,
1012 eaar3213.

1013 Schneider, F.D., Morsdorf, F., Schmid, B., Schimel, D.S., Schaepman, M.E., Petchey, O.L., *et*
1014 *al.* (2017). Mapping functional diversity from remotely sensed morphological and
1015 physiological forest traits. *Nat. Commun.*, 8.

1016 Sitters, J., Atkinson, C.L., Guelzow, N., Kelly, P. & Sullivan, L.L. (2015). Spatial stoichiometry:

1017 Cross-ecosystem material flows and their impact on recipient ecosystems and organisms.
1018 *Oikos*, 124, 920–930.

1019 Sobral, M., Silviu, K.M., Overman, H., Oliveira, L.F.B., Raab, T.K. & Fragoso, J.M.V. (2017).
1020 Mammal diversity influences the carbon cycle through trophic interactions in the Amazon.
1021 *Nat. Ecol. Evol.*, 1, 1670–1676.

1022 Somveille, M., Manica, A. & Rodrigues, A.S.L. (2019). Where the wild birds go: explaining the
1023 differences in migratory destinations across terrestrial bird species, 225–236.

1024 Somveille, M., Rodrigues, A.S.L. & Manica, A. (2018). Energy efficiency drives the global
1025 seasonal distribution of birds. *Nat. Ecol. Evol.*, 2, 962–969.

1026 Strandburg-Peshkin, A., Farine, D.R., Couzin, I.D. & Crofoot, M.C. (2015). Shared decision-
1027 making drives collective movement in wild baboons. *Science (80-.)*, 348, 1358–1361.

1028 Strandburg-Peshkin, A., Farine, D.R., Crofoot, M.C. & Couzin, I.D. (2017). Habitat and social
1029 factors shape individual decisions and emergent group structure during baboon collective
1030 movement. *Elife*, 6.

1031 Stuart, M.B., McGonigle, A.J.S. & Willmott, J.R. (2019). Hyperspectral Imaging in Environmental
1032 Monitoring: A Review of Recent Developments and Technological Advances in Compact
1033 Field Deployable Systems. *Sensors (Basel)*, 19, 3071.

1034 Subalusky, A.L., Dutton, C.L., Rosi-Marshall, E.J. & Post, D.M. (2015). The hippopotamus
1035 conveyor belt: vectors of carbon and nutrients from terrestrial grasslands to aquatic
1036 systems in sub-Saharan Africa. *Freshw. Biol.*, 60, 512–525.

1037 Subalusky, A.L., Dutton, C.L., Rosi, E.J. & Post, D.M. (2017). Annual mass drownings of the
1038 Serengeti wildebeest migration influence nutrient cycling and storage in the Mara River.
1039 *Proc. Natl. Acad. Sci.*, 114, 7647 LP-7652.

1040 Subalusky, A.L. & Post, D.M. (2018). Context dependency of animal resource subsidies. *Biol.*
1041 *Rev.*

1042 Thorson, J.T., Scheuerell, M.D., Shelton, A.O., See, K.E., Skaug, H.J. & Kristensen, K. (2015).
1043 Spatial factor analysis: a new tool for estimating joint species distributions and correlations
1044 in species range. *Methods Ecol. Evol.*, 6, 627–637.

1045 van Toor, M.L., O'Mara, M.T., Abedi-Lartey, M., Wikelski, M., Fahr, J. & Dechmann, D.K.N.
1046 (2019). Linking colony size with quantitative estimates of ecosystem services of African
1047 fruit bats. *Curr. Biol.*, 29, R237–R238.

1048 Tsalyuk, M., Kilian, W., Reineking, B. & Getz, W.M. (2019). Temporal variation in resource
1049 selection of African elephants follows long-term variability in resource availability. *Ecol.*
1050 *Monogr.*, 89, e01348.

1051 Tucker, M.A., Böhning-Gaese, K., Fagan, W.F., Fryxell, J.M., Van Moorter, B., Alberts, S.C., *et*
1052 *al.* (2018). Moving in the Anthropocene: Global reductions in terrestrial mammalian
1053 movements. *Science* (80-.).

1054 Vanni, M.J. (2002). N UTRIENT C YCLING B Y A NIMALS IN F RESHWATER E COSYSTEMS.

1055 Wang, Y., Nickel, B., Rutishauser, M., Bryce, C.M., Williams, T.M., Elkaim, G., *et al.* (2015).
1056 Movement, resting, and attack behaviors of wild pumas are revealed by tri-axial
1057 accelerometer measurements. *Mov. Ecol.*, 3, 2.

1058 Weathers, K.C., Strayer, D.L. & Likens, G.E. (2012). *Fundamentals of ecosystem science*.
1059 *Fundam. Ecosyst. Sci.*

1060 Wegmann, M. (2017). Remote Sensing Training in Ecology and Conservation – challenges and
1061 potential. *Remote Sens. Ecol. Conserv.*, 3, 5–6.

1062 Wenger, S.J., Subalusky, A.L. & Freeman, M.C. (2019). The missing dead: The lost role of
1063 animal remains in nutrient cycling in North American Rivers. *Food Webs*, 18, e00106.

1064 West, J.B., Bowen, G.J., Dawson, T.E. & Tu, K.P. (2010). *Isoscapes: Understanding movement,*
1065 *pattern, and process on earth through isotope mapping. Isoscapes Underst. Movement,*
1066 *Pattern, Process Earth Through Isot. Mapp.*

1067 Wilcove, D.S. & Wikelski, M. (2008). Going, Going, Gone: Is Animal Migration Disappearing.
1068 *PLoS Biol.*, 6, e188.

1069 Williams, T.M., Wolfe, L., Davis, T., Kendall, T., Richter, B., Wang, Y., *et al.* (2014).
1070 Instantaneous energetics of cougar kills reveals advantage of felid sneak attacks. *Science*
1071 (80-.), 17331, 1–18.

1072 Wilmers, C.C., Nickel, B., Bryce, C.M., Smith, J.A., Wheat, R.E. & Yovovich, V. (2015). The
1073 golden age of bio-logging: how animal-borne sensors are advancing the frontiers of
1074 ecology. *Ecology*, 96, 1741–1753.

1075 Wilson, R.P., Börger, L., Holton, M.D., Scantlebury, D.M., Gómez-Laich, A., Quintana, F., *et al.*
1076 (2020). Estimates for energy expenditure in free-living animals using acceleration proxies:
1077 A reappraisal. *J. Anim. Ecol.*, 89, 161–172.

1078 Wilson, R.P., WHITE, C.R., QUINTANA, F., HALSEY, L.G., LIEBSCH, N., MARTIN, G.R., *et al.*
1079 (2006). Moving towards acceleration for estimates of activity-specific metabolic rate in free-
1080 living animals: the case of the cormorant. *J. Anim. Ecol.*, 75, 1081–1090.

1081 Winner, K., Noonan, M.J., Fleming, C.H., Olson, K.A., Mueller, T., Sheldon, D., *et al.* (2018).
1082 Statistical inference for home range overlap. *Methods Ecol. Evol.*, 9, 1679–1691.

1083 Xie, H., Luo, X., Xu, X., Pan, H. & Tong, X. (2016). Automated subpixel surface water mapping
1084 from heterogeneous urban environments using Landsat 8 OLI imagery. *Remote Sens.*, 8,

1085 1–16.
1086 Zellweger, F., Coomes, D., Frenne, P. De, Lenoir, J. & Rocchini, D. (2018). Advances in
1087 Microclimate Ecology Arising from Remote Sensing. *Trends Ecol. Evol.*, 1–15.
1088